Phosphate (Pi) stress-responsive transcription factors PdeWRKY6 and PdeWRKY65 regulate the expression of PdePHT1;9 to modulate tissue Pi concentration in poplar

Phosphate (Pi) stress-responsive transcription factors PdeWRKY6 and PdeWRKY65 regulate the expression of *PdePHT1;9* to modulate tissue Pi concentration in poplar

Xiaoqing Yang [1], Keai Zhang [1], Tashbek Nvsvrot [1], Yan Zhang [1], Guanghua Cai [1], Liyu Huang [1], Wenyu Ren [1], Yiwei Ding [1], John P Hammond [2], Lei Shi [3], Nian Wang [1, 4, *]

[1] College of Horticulture and Forestry Sciences, Huazhong Agricultural University, Wuhan, 430070, China; [2] School of Agriculture, Policy and Development, University of Reading, Reading RG6 6AR, UK; [3] College of Resources and Environment, Huazhong Agricultural University, Wuhan, 430070, China; [4] Hubei Engineering Technology Research Center for Forestry Information, Huazhong Agricultural University, Wuhan, 430070, China

[*] Corresponding author

Email Address:

Xiaoqing Yang: 504147986@qq.com

Keai Zhang: zhangkeai20@outlook.com

Tashbek Nvsvrot: Tashbek@163.com

Yan Zhang: mint_19@163.com

Guanghua Cai: Cai_911@yeah.net

Liyu Huang: 69460929@qq.com

Wenyu Ren: wenyu_ren@163.com

Yiwei Ding: 1746554731@qq.com

John P Hammond: j.p.hammond@reading.ac.uk

Lei Shi: leish@mail.hzau.edu.cn

Nian Wang: wangn@mail.hzau.edu.cn

Correspondence to: Nian Wang, College of Horticulture and Forestry Sciences, Huazhong Agricultural University, Wuhan, 430070, China; Fax: (86)27-87282010; Tel: (86)-18627000091; ORCID: 0000-0001-9185-4199

With 9 figures and 0 table

Word count (5941): Introduction, 883; M&M, 1834; results, 2278; Discussions, 946

Running title: WRKY65 and WRKY6 regulates Pi content in poplar

SUMMARY

Phosphorus (P) is an important nutrient for plants. Here, we identify a WRKY transcription factor (TF) in poplar (*Populus deltoides* × *Populus euramericana*) (PdeWRKY65) that modulates tissue phosphate (Pi) concentrations in poplar. PdeWRKY65 overexpression (OE) transgenic lines showed reduced shoot Pi concentrations under both low and normal Pi availabilities, while PdeWRKY65 reduced expression (RE) lines showed the opposite phenotype. A gene encoding a Pi transporter (PHT), PdePHT1;9, was identified as the direct downstream target of PdeWRKY65 by RNA sequencing (RNA-Seq). The negative regulation of PdePHT1;9 expression by PdeWRKY65 was confirmed by DNA–protein interaction assays, including yeast one-hybrid (Y1H), electrophoretic mobility shift assay (EMSA), co-expression of the promoters of PdePHT1;9 and PdeWRKY65 in tobacco (*Nicotiana benthamiana*) leaves, and chromatin immunoprecipitation–quantitative PCR. A second WRKY TF, PdeWRKY6, was subsequently identified and confirmed to positively regulate the expression of PdePHT1;9 by DNA–protein interaction assays. PdePHT1;9 and PdeWRKY6 OE and RE poplar transgenic lines were used to confirm their positive regulation of shoot Pi concentrations, under both normal and low Pi availabilities. No interaction between PdeWRKY6 and PdeWRKY65 was observed at the DNA or protein levels. Collectively, these data suggest that the low Pi-responsive TFs PdeWRKY6 and PdeWRKY65 independently regulate the expression of PHT1;9 to modulate tissue Pi concentrations in poplar.

INTRODUCTION

Phosphorus (P) is one of the most important nutrients for plant growth and development. Plants take up P in the form of phosphate (Pi) from the rhizosphere through several different transporters (Raghothama, 1999). In plant cells, Pi concentrations are typically greater than 10 mm (Raghothama, 1999), while there is usually less than 10 μm Pi available in the soil solution (Bieleski, 1973; Shen et al., 2011), creating the need for active transport of Pi across the plasma membrane by specialized transporters.

Globally, approximately 70% of cultivated land suffers from low Pi availability (Lopez-Arredondo et al., 2014). Plants have evolved a complex regulatory network to overcome the low availability of Pi in many soils. In recent decades, significant advances have been made in elucidating plant uptake and regulation mechanisms (Bucher, 2007; Lopez-Arredondo et al., 2014; Shen et al., 2011). However, there is still a lack of knowledge around the regulation of multiple genes in response to low Pi stress, especially in perennial tree plants.

Pi transporters of the PHT1 family are responsible for Pi uptake and transportation (Bucher, 2007; Remy et al., 2012; Ren et al., 2014). Most of the genes in this family in Arabidopsis are expressed in roots and their expression is responsive to low Pi availability (Mudge et al., 2002b). The expression of some members was also found in shoots, stems, and flowers (Misson et al., 2005; Mudge et al., 2002b). However, some members of the PHT1 family, such as AtPHT1;8 and AtPHT1;9, were also reported to translocate Pi from roots to shoots (Lapis-Gaza et al., 2014; Misson et al., 2005). AtPHT1;5 was found to play a critical role in mobilizing Pi from P source to sink organs in accordance with developmental cues and plant P status (Nagarajan et al., 2011). In rice (*Oryza sativa*), OsPHT1;1 was shown to modulate Pi uptake and translocation in Pi-replete conditions (Sun et al., 2012). These results demonstrate that in plants, Pi transporters of the PHT1 family are involved in Pi uptake and plant P responses in diverse ways. In silico analyses of various plant genomes revealed 9, 14, 14, and 8 PHT1 genes in Arabidopsis, apple (*Malus domestica*), poplar (*Populus trichocarpa*), and tomato (*Solanum lycopersicum*) (Chen et al., 2014; Mudge et al., 2002a; Sun et al., 2017; Zhang, Meng, et al., 2016), respectively. Although the identification of PHT1 genes in poplar has been conducted, their functions in Pi uptake and regulation remain unknown.

A number of transcription factors (TFs) have been shown to play important roles in the regulation of plant responses to low Pi availability, especially members of the WRKY TF family (Gu et al., 2016). In the model plant Arabidopsis, AtWRKY45 activates the expression of AtPHT1;1 by directly binding to the W-Box (core bases, TTGAC[C/T])

in the promoter of AtPHT1;1 in response to low Pi availability (Wang et al., 2014). Separately, AtWRKY42 negatively regulates phosphate1 (PHO1) expression by binding to the AtPHO1 promoter under Pi-replete conditions, whilst under Pi-deficient conditions, AtWRKY42 is degraded through the 26S proteasome pathway (Su et al., 2015). The expression of AtPHT1;1 has also been shown to be positively regulated by AtWRKY42 (Su et al., 2015). The different regulatory effects of AtWRKY42 on AtPHO1 and AtPHT1;1 resulted in a complex regulatory network for plant Pi status. AtWRKY6 was also shown to be involved in the regulation of Arabidopsis responses to low Pi availability by modulating the expression of AtPHO1 (Chen et al., 2009). Further study revealed that the degradation of AtWRKY6 during low Pi availability was executed by a ubiquitin E3 ligase, Pi response ubiquitin E3 ligase1 (PRU1) (Ye et al., 2018). AtWRKY75 was also shown to act as a modulator of Pi uptake and root development in Arabidopsis (Devaiah et al., 2007). In rice, OsWRKY74 modulates tolerance to low Pi availability, possibly through modifying the root system architecture (Dai et al., 2016). This evidence suggests that members of the WRKY TF family in plants play important roles in the regulation of Pi uptake, Pi translocation, and tissue Pi status.

Poplar (*Populus* spp.) is a model plant for tree species due to its fast growth, small genome, and easy genetic transformation. However, there is very limited knowledge on how poplar responds to low Pi availability at the molecular level. Thus, there is a need to understand the molecular mechanisms involved in responses to low Pi availability in poplar. In our previous study, transgenic PdeWRKY65 overexpression (OE) and reduced expression (RE) lines were generated. In this study, we observed that the PdeWRKY65 OE transgenic lines showed Pi-deficient symptoms when they were grown under both low and normal Pi availabilities, while PdeWRKY65 RE lines showed the opposite phenotype. To investigate how PdeWRKY65 regulates tissue Pi concentrations in poplar, its downstream gene PdePHT1;9 was identified and confirmed. Moreover, a second WRKY TF, PdeWRKY6, was also identified and confirmed to be involved in the regulation of Pi concentrations via the control of the expression of PdePHT1;9. The dual regulation of PdePHT1;9 by two WRKY members may enable

greater control over tissue Pi status in poplar under low Pi availability. We have uncovered a novel pathway for the regulation of tissue Pi concentrations under Pi deficiency in woody plants, enhancing our understanding of the regulation of Pi concentrations in plants.

RESULTS

Overexpression of PdeWRKY65 reduced shoot Pi concentrations in poplar and Arabidopsis

In our previous study, PdeWRKY65 OE transgenic lines in poplar (*Populus deltoides* × *Populus euramericana*), W65-OE1, W65-OE2, and W65-OE3, were generated and they were used to characterize its function. In these three lines, the expression of PdeWRKY65 was increased 276.5±14.5, 228.6±27.9, and 205.3±20.6 times compared with the wild type (WT), respectively. Growth of the PdeWRKY65 OE transgenic lines W65-OE1, W65-OE2, and W65-OE3 in soil with normal irrigation was inhibited compared with the WT (Figure 1a,b). Plant height and the 6th internode diameter were significantly shorter in the three OE lines compared to the WT ($P < 0.05$) (Figure 1c,d). Moreover, the three OE lines showed visible red shoots, while no colour change was observed in WT. This symptom was consistent with plants growing under low Pi availability. Interestingly, root Pi concentrations of the three OE transgenic lines were equal to or significantly higher than WT levels (Figure 1e); in contrast, shoot Pi concentrations of the three OE transgenic lines were significantly lower than WT levels (Figure 1e). The higher root Pi concentrations and reduced shoot Pi concentrations suggested that Pi translocation from roots to shoots might be reduced in the PdeWRKY65 OE transgenic lines. In soil with a low Pi availability, the growth inhibition and Pi deficiency symptoms in the three OE lines were stronger (Figure S1). The shoots in the OE lines were much redder. Plant heights of the three OE lines were significantly reduced compared with WT, while the root length showed no significant difference between WT and OE lines. Root and shoot Pi concentrations of the three OE lines were significantly lower than WT levels (Figure S1) ($P < 0.05$). These data still

155 support a reduction in the translocation of Pi from the roots to shoots in the
156 PdeWRKY65 OE transgenic lines.
157
158 Meanwhile, two independent transgenic lines with heterologous PdeWRKY65 OE in
159 Arabidopsis were generated (Figure S2a) and confirmed by PCR and reverse
160 transcriptase-PCR (RT-PCR) (Figure S2b,c). Both of these OE lines harboured one
161 introduced homozygous 2×35S::PdeWRKY65 copy in their genomes, confirmed by a
162 3:1 segregation ratio for the selected marker in the T2 generation (see Experimental
163 Procedures). When the two OE T3 generation lines were grown on MS medium and
164 soil, both of them showed visible growth reductions (Figure S2a,d). The roots of the
165 two PdeWRKY65 OE lines on MS medium were significantly shorter than WT roots
166 ($P < 0.05$) (Figure S2e). When grown in Pi-replete soil, root Pi concentrations in both
167 OE transgenic lines were significantly higher than in WT levels, while shoot Pi
168 concentrations of both OE transgenic lines were significantly lower than WT levels
169 (Figure S2f,g). These data are consistent with observations in PdeWRKY65 OE poplar
170 and suggest that PdeWRKY65 negatively regulates Pi translocation from roots to
171 shoots.
172
173 **Reduced expression of PdeWRKY65 in poplar enhanced Pi translocation to shoots**
174 **and expression of PdeWRKY65 is inhibited by low Pi availability**
175
176 PdeWRKY65 RE transgenic lines, W65-RE2 and W65-RE3, were also generated. The
177 expression levels of PdeWRKY65 in these two lines were reduced to 51 and 27%
178 compared with WT levels, respectively. When grown under Pi-replete conditions in
179 woody plant medium (WPM) and soil, the PdeWRKY65 RE transgenic lines, W65-
180 RE2 and W65-RE3, showed no difference in growth or shoot or root Pi concentrations
181 (data not shown). When the PdeWRKY65 RE transgenic lines were grown in WPM
182 with low Pi availability (0.125 mm Pi) for 15 days, both the transgenic and WT lines
183 also showed no difference in growth of aboveground parts (Figure 2a,b). However,
184 roots of the two PdeWRKY65 RE transgenic lines were significantly longer than WT
185 roots (Figure 2c) ($P < 0.05$). The root Pi concentrations of the two PdeWRKY65 RE

lines, W65-RE2 and W65-RE3, were significantly lower than WT levels ($P < 0.05$), and the shoot Pi concentrations of these two RE lines were significantly higher (Figure 2d,e).

To further examine the role of PdeWRKY65 in Pi regulation in poplar, its expression in WT was examined after 10 days of growth under low Pi availability. The expression of PdeWRKY65 was lower in both roots and shoots compared to normal Pi availability (Figure S3a). These data, together with the observations in PdeWRKY65 OE and RE transgenic lines in poplar and Arabidopsis, suggest that PdeWRKY65 is involved in plant responses to low Pi availability and negatively regulates Pi translocation to shoots in poplar.

PdePHT1;9 is a downstream gene of PdeWRKY65 in response to low Pi stress

To identify which genes operate downstream of PdeWRKY65 in response to low Pi availability, RNA-Seq analysis was performed on PdeWRKY65 OE and WT lines. Clustering of all samples suggested that the RNA-Seq experiment was performed well and it could be used in further analysis (Figure S3b). A total of 3253 genes showed differential expression between WT and OE lines (Table S2). As expected, PdeWRKY65 showed a significantly higher transcript abundance compared to WT. Among the 3253 differentially expressed genes, Potri.005G256100 showed a high similarity to PHT1;9 in Arabidopsis. Therefore, it is named PdePHT1;9 in this study (Figure 3a). In previous reports, PHT1;9 was demonstrated to be involved in Pi uptake and translocation (Lapis-Gaza et al., 2014; Remy et al., 2012). The expression of PdePHT1;9 was approximately 40% lower in PdeWRKY65 OE compared with WT lines, and these expression patterns agreed with the phenotype of Pi deficiency observed in PdeWRKY65 OE lines (Table S2). This suggests that PdePHT1;9 may act downstream of PdeWRKY65 in the response to low Pi availability.

To test this, the expression of PdePHT1;9 was first examined by qRT-PCR. After 10 days of growth under low Pi availability, the expression of PdePHT1;9 was increased in both shoots and roots compared to growth under normal Pi availability (Figure 3b).

Tissue analysis revealed that PdePHT1;9 expression was higher in leaves than in other tissues (Figure 3c). Additionally, the expression of PdePHT1;9 was reduced in PdeWRKY65 OE lines, while its expression was increased in PdeWRKY65 RE lines under normal Pi availability (Figure 3d). The expression of AtPHT1;9 was also reduced in PdeWRKY65 OE transgenic Arabidopsis lines (Figure S2h), while AtPHO1 expression did not show any change (Figure S2i). To comprehensively investigate the expression pattern of PdePHT1;9, its promoter was fused with the GUS-encoding gene (Figure 3e). Within the 1480-bp promoter sequence, three W-Box motifs were identified, located at −246, −528, and −916 bp relative to the position of the start codon (Data S1). Under normal Pi availability, the PdePHT1;9::GUS transgenic lines showed visible staining in leaves, the root apex, and cambium. Interestingly, the mature leaves were darker blue than young leaves (Figure 3e). Under low Pi availability, the PdePHT1;9::GUS transgenic lines were stained much darker blue in leaves and roots (Figure 3e).

To support the interaction between PdeWRKY65 and the promoter of PdePHT1;9, a positive interaction was demonstrated by Y1H (Figure 4a). Co-expression of 35S::PdeWRKY65 and PdePHT1;9::LUC or PdePHT1;9::GUS in tobacco leaves both showed that PdeWRKY65 inhibited the expression of PdePHT1;9 (Figure 4b,c). EMSA revealed that PdeWRKY65 could bind to the W-Box in the promoter of PdePHT1;9 (Figure 4d). A chromatin immunoprecipitation (ChIP) experiment was performed using 35S::PdeWRKY65:Flag- and 35S::Flag-transformed hairy roots. Quantitative PCR (qPCR) analysis revealed that when using an anti-Flag antibody in 35S::PdeWRKY65:Flag-transformed hairy roots, W-Box fragments within the promoter of PdePHT1;9 were immunoprecipitated (Figure 4e). These data demonstrate that PdeWRKY65 can bind to the W-Box motifs located at −246 and −528 bp of the PdePHT1;9 promoter in vivo. The binding activities of PdeWRKY65 to these two W-Box motifs were different according to the relative abundance of immunoprecipitated DNA (Figure 4e). Collectively, both in vivo and in vitro protein–DNA interaction assays revealed that PdeWRKY65 directly inhibits the expression of PdePHT1;9 by binding to W-Box motifs within its promoter.

PdePHT1;9 is a positive regulator of Pi translocation in poplar

To investigate the function of PdePHT1;9, PdePHT1;9 OE and RE transgenic lines were generated in poplar (Figure S4a,b). PCR analysis, GUS staining, and qRT-PCR-based confirmation of the introduced genes/fragments in the transgenic lines all indicated that PdePHT1;9 OE and RE lines were successfully generated (Figure S4c–g). Three OE lines, PHT-OE3, PHT-OE4, and PHT-OE5, and two RE lines, PHT-RE1 and PHT-RE2, were selected for further analyses.

When grown on WPM with normal Pi availability for 15 days, the three PdePHT1;9 OE lines showed visibly more biomass than WT (Figure 5a). The root Pi concentrations were significantly lower in the PdePHT1;9 OE lines compared to WT and the shoot Pi concentrations were significantly higher than WT levels ($P < 0.05$) (Figure 5b,c). In contrast, the two PdePHT1;9 RE lines showed a visible growth reduction compared to WT under normal Pi availability (Figure 5d). Root Pi concentrations in the two PdePHT1;9 RE lines were significantly higher than WT levels, and the shoot Pi concentrations were significantly lower than WT levels ($P < 0.05$) (Figure 5e,f). These data suggest that PdePHT1;9 has a positive role in Pi translocation from roots to shoots in poplar under normal Pi conditions. Under low Pi availability, the OE and RE transgenic lines showed similar patterns of tissue Pi concentrations (Figure 5g–l), with the exception of the root Pi concentrations in the OE lines, which were significantly higher than WT levels (Figure 5k,l). Considering PdePHT1;9 is a downstream target of PdeWRKY65, PdeWRKY65 negatively regulates Pi translocation, and both genes can respond to low Pi availability, we speculate that the PdeWRKY65–PdePHT1;9 gene module enhances Pi translocation to shoots in poplar under low Pi availability.

The expression of PdeWRKY6 was activated upon low Pi stress and it directly regulated the expression of PdePHT1;9.

In the RNA-Seq analysis of PdeWRKY65 OE transgenic lines, we also identified

Potri.002G228400, whose expression was also increased and has high similarity to AtWRKY6 (Table S2). Phylogenetic analysis showed that PdeWRKY6 had the shortest phylogenetic distance to AtWRKY6, AtWRKY42, and AtWRKY31 (Figure 6a). AtWRKY6 and AtWRKY42 have previously been shown to be involved in Pi regulation in Arabidopsis (Chen et al., 2009; Su et al., 2015). The subcellular location of PdeWRKY6 in tobacco leaf showed it was located in the nucleus (Figure 6b). The expression of PdeWRKY6 in PdeWRKY65 OE and RE transgenic lines showed increased expression in OE and reduced expression in PdeWRKY65 RE lines (Figure 6c). PdeWRKY6 showed higher expression in leaf and root compared to other tissues (Figure 6d), and growth under low Pi availability for 10 days increased PdeWRKY6 expression in both roots and shoots (Figure 6e). The expression of PdeWRKY6 in PdeWRKY65 OE and RE transgenic lines suggested that PdeWRKY65 might positively regulate the expression of PdeWRKY6, while their expression under low Pi stress suggested that PdeWRKY65 might negatively regulate the expression of PdeWRKY6. This inconsistency suggested that PdeWRKY6 might not be a downstream target of PdeWRKY65.To investigate the role of PdeWRKY6 in Pi regulation, OE and RE transgenic lines were generated for this gene in poplar (Figure S5a,b). Three OE lines, W6-OE1, W6-OE2, and W6-OE3, and five RE lines, W6-RE1 to W6-RE5, were selected for further analyses (Figure S5c–g). The expression of PdePHT1;9 in PdeWRKY6 OE and RE transgenic lines was increased and reduced in PdeWRKY6 OE and RE transgenic lines, respectively (Figure 6f). Our Y1H assay revealed that PdeWRKY6 could bind to the promoter of PdePHT1;9 in yeast (Figure 6g), and co-expression of 35S::PdeWRKY6 and PdePHT1;9::GUS or PdePHT1;9::LUC in tobacco leaves showed that PdeWRKY6 activated the expression of PdePHT1;9 (Figure 6h,i). A ChIP-qPCR experiment was also performed, showing that PdeWRKY6 could bind to the W-Box motif located at −916 bp of the PdePHT1;9 promoter in vivo (Figure 6j). More specifically, EMSA revealed that PdeWRKY6 could bind to the W-Box in the promoter of PdePHT1;9 (Figure 6k). Collectively, these data suggest that PdeWRKY6 positively regulates the expression of PdePHT1;9 by directly binding to the W-Box within its promoter.

PdeWRKY6 is a positive regulator of Pi concentrations in poplar

To test the functional role of PdeWRKY6 in Pi regulation, the OE and RE transgenic lines were grown in WPM with normal Pi availability for 15 days. There was no visible growth difference between WT and transgenic lines. However, root Pi concentrations were significantly lower in PdeWRKY6 OE compared to the WT ($P < 0.05$) (Figure S6a); in contrast, shoot Pi concentrations were significantly higher in PdeWRKY6 OE compared to the WT ($P < 0.05$) (Figure S6b). In PdeWRKY6 RE lines, root and shoot Pi concentrations showed opposite trends to PdeWRKY6 OE lines (Figure S6c,d). Subsequently, two OE lines, W6-OE1 and W6-OE2, and two RE lines, W6-RE2 and W6-RE3, were grown in WPM with low Pi availability for 15 days. The two OE lines showed a visibly better growth performance than WT, and both roots and shoots had significantly higher Pi concentrations compared to WT ($P < 0.05$) (Figure 7a–c). In contrast, the two RE lines showed weaker growth than WT, and both roots and shoots had significantly lower Pi concentrations compared to WT (Figure 7d–f), although this difference was not significant for the root Pi concentration in W6-RE2. Consequently, we suggest that PdeWRKY6 is a positive regulator of root and shoot Pi concentrations in poplar. Considering the regulation of Pi concentrations by PdePHT1;9 and the direct activation of PdePHT1;9 expression by PdeWRKY6, we also suggest that PdeWRKY6 positively regulates the expression of PdePHT1;9 and they form a gene module, PdeWRKY6–PdePHT1;9, to regulate tissue Pi concentrations in poplar.

PdeWRKY6 and PdeWRKY65 regulate the expression of PdePHT1;9 independently

It is possible that PdeWRKY6 and PdeWRKY65 interact with each other and that this interaction is involved in the regulation of PdePHT1;9 expression. However, using a Y2H assay, no interaction between PdeWRKY6 and PdeWRKY65 was observed (Figure S7a). We hypothesized that PdeWRKY65 might also positively regulate the expression of PdeWRKY6 according to the expression analysis in PdeWRKY65 OE and RE lines (Figure 6c). However, this is not supported by the data for these TFs under

low Pi stress (Figure 6e). Co-expression of PdeWRKY6::GUS or PdeWRKY6::LUC and 35S::PdeWRKY65 in tobacco leaves also revealed that there was no direct activation or inhibition of PdeWRKY6 expression by PdeWRKY65 (Figure S7b,c). Additionally, it is also possible that PdeWRKY65 is a downstream gene of PdeWRKY6. Thus, the expression of PdeWRKY65 in PdeWRKY6 OE and RE lines was also examined by qRT-PCR. The data revealed no clear trend for the expression of PdeWRKY65 in PdeWRKY6 OE and RE lines, although the expression of PdeWRKY65 was reduced in all PdeWRKY6 RE lines (Figure S7d). Thus, these expression patterns did not support the hypothesis that PdeWRKY65 is a downstream gene of PdeWRKY6. Collectively, these data suggest that PdeWRKY6 and PdeWRKY65 regulate the expression of PdePHT1;9 in response to low Pi stress without direct interaction.

DISCUSSION

Dual regulation of PdePHT1;9 by PdeWRKY65 and PdeWRKY6 ensures Pi can be translocated to shoots under low Pi conditions

The expression of all three genes, PdeWRKY65, PdeWRKY6, and PdePHT1;9, was altered in response to low Pi availability. After 10 days under low Pi availability, the expression of PdeWRKY6 and PdePHT1;9 was increased (Figures 6e and 3b), while the expression of PdeWRKY65 was decreased (Figure S3a). Moreover, both PdeWRKY65 and PdeWRKY6 could bind to independent W-Box motifs in the promotor of PdePHT1;9 and therefore regulate the expression of PdePHT1;9. However, these two WRKY TFs regulate the expression of PdePHT1;9 with different patterns; PdeWRKY65 inhibited PdePHT1;9 expression (Figure 3d), while PdeWRKY6 activated PdePHT1;9 expression under low Pi availability (Figure 6f). According to our ChIP-qPCR results, PdeWRKY65 can bind the W-Box motifs located at −246 and −528 bp of the PdePHT1;9 promoter (Figure 4e), while PdeWRKY6 can only bind the W-Box motif located at −916 bp (Figure 6g). These different binding patterns may be attributed to the different regulation of PdePHT1;9 by the two TFs. Based on these

data, we propose a regulatory model of PdeWRKY65, PdeWRKY6, PdePHT1;9, and Pi transport to shoots in poplar (Figure 8).

In this model, PdeWRKY65 and PdeWRKY6 work separately to regulate the expression of PdePHT1;9 under low Pi availability, resulting in increased PdePHT1;9 expression and enhanced Pi translocation to the shoots. The two different regulatory patterns provide some redundancy to the system facilitating Pi translocation. Moreover, the two different regulation patterns may also enable greater Pi translocation to shoots under low Pi availability. Therefore, the expression of PdePHT1;9 separately regulated by PdeWRKY65 and PdeWRKY6 suggests that plants have evolved dual strategies to ensure sufficient Pi can be translocated to shoots under low Pi availability. This double-guarantee regulation strategy has also been reported in other biological processes in plants, such as dual regulation of gene expression mediated by MAPK and salicylic acid to enhance innate immunity in Arabidopsis (Tsuda et al., 2013).

Under normal Pi availability, the expression of PdeWRKY65 and PdeWRKY6 was relatively high in roots (Figure 6d). This suggests that the expression of PdePHT1;9 is also regulated by both PdeWRKY65 and PdeWRKY6 under normal Pi availability. Considering PdeWRKY65 and PdeWRKY6 regulate the expression of PdePHT1;9 by opposing strategies, there is potential to tightly regulate the expression of PdePHT1;9 in poplar. This regulation might enable a close regulation of tissue Pi concentrations in poplar, ensuring normal growth for plants under normal Pi availability.

Complex functions of PdePHT1;9 in regulating tissue Pi concentrations

PHT1 genes have previously been reported to play roles in both Pi assimilation and translocation (Nagarajan et al., 2011; Remy et al., 2012; Ren et al., 2014). In this study, PHT1;9 OE in poplar increased shoot Pi concentrations under both normal and low Pi availabilities, while root Pi concentrations were decreased and increased under normal and low Pi availabilities, respectively (Figure 5b,c,h,i). Transgenic PdePHT1;9 RE lines in poplar showed opposite patterns of shoot and root Pi concentrations (Figure 5e,f,k,l).

According to these data, we could speculate that PdePHT1;9 positively regulates Pi translocation from roots to shoots under normal Pi availability. However, we also noted that the root Pi concentrations in the PdePHT1;9 OE lines were significantly lower than WT levels in normal Pi conditions and higher in low Pi conditions (Figure 5b,h). These data suggest that PdePHT1;9 might also regulate Pi uptake when its expression is relatively high under low Pi availability. In PdeWRKY65 RE lines, the expression of PdePHT1;9 was only increased approximately 2.0- to 2.5-fold (Figure 3d); thus, the PdeWRKY65 RE lines did not show increased uptake in roots. Additionally, the root Pi concentration was also increased in PdeWRKY6 OE lines under low Pi availability, and this also supports our hypothesis. These observations are consistent with the functions of PHT1;9 in other plants (Remy et al., 2012; Wang et al., 2021).

In plants, nutrients are recycled from senescent leaves to young tissues (Guo et al., 2021). Thus, Pi may be relocated from old leaves to shoots that require Pi for development (Stigter & Plaxton, 2015). The plasma membrane transporter OsPHO1;2 has previously been shown to play a role in reallocation of Pi from leaves to seeds in rice (Ma et al., 2021), and another PHT1 member, OsPHT1;8, translocates Pi from the panicle axis to the grain (Jia et al., 2011). In this study, in the PdePHT1;9::GUS transgenic lines, the data revealed higher relative expression in mature/aging leaves compared to young leaves (Figure 3e). We also showed that PdePHT1;9 could positively regulate Pi translocation from roots to shoots in poplar. We therefore suggest that PdePHT1;9 may also regulate Pi translocation from mature leaves to shoots. However, further evidence is required to support this.

In Arabidopsis, PHO1 is expressed in cells of the vascular system of roots and it has been shown to be involved in the translocation of Pi from the root to the shoot through loading Pi to xylem (Hamburger et al., 2002). Its regulators, AtWRKY6 and AtWRKY42, also showed expression in roots and stems (Su et al., 2015; Ye et al., 2018). The Arabidopsis Pht1;9 gene is highly expressed in Pi-starved roots and plays roles in Pi acquisition (Remy et al., 2012). Here, under normal Pi availability, the PdePHT1;9::GUS transgenic lines showed visible staining in leaves, the root apex, and

cambium (Figure 3e), while under low Pi availability, the PdePHT1;9::GUS transgenic lines were stained much darker blue in leaves and roots (Figure 3e). We hypothesized that PdePHT1;9 is involved in Pi translocation and uptake. Considering its functions and the similar expression patterns under both normal and low Pi availability to PHO1 and PHT1;9 in Arabidopsis, we also speculate that PdePHT1;9 might translocate phosphate from roots to shoots through loading Pi to xylem. Moreover, PdePHT1;9 is expressed in the root apex, in agreement with its roles in Pi uptake.

PdeWRKY6 may also regulate Pi uptake in roots under low Pi availability

Under normal Pi availability, root Pi concentrations were lower in PdeWRKY6 OE transgenic lines compared to WT lines, while shoot Pi concentrations were higher in PdeWRKY6 OE transgenic lines (Figure S6a,b). In contrast, PdeWRKY6 RE transgenic lines showed an opposite trend (Figure S6c,d). These data suggest that PdeWRKY6 positively regulates Pi translocation from roots to shoots under normal Pi availability. However, under low Pi availability, root and shoot Pi concentrations were higher in PdeWRKY6 OE transgenic lines compared to WT lines (Figure 7b,c), while PdeWRKY6 RE transgenic lines showed an opposite trend (Figure 7e,f). These data suggest that PdeWRKY6 positively regulates root and shoot Pi concentrations under low Pi availability, either directly or indirectly, by altering the tissue Pi source–sink relationships between roots and shoots. These patterns were partially different from Pi concentrations in PdeWRKY65 OE and RE transgenic lines. PdeWRKY65 showed positive regulation of shoot Pi concentrations, but not root Pi concentrations. Therefore, these data may suggest that PdeWRKY6 may not only regulate Pi translocation to shoots, but also Pi uptake in poplar roots under low Pi availability. We already speculated that PdePHT1;9 might also regulate Pi uptake when its expression is relatively high under low Pi availability. Thus, PdePHT1;9 is also a downstream target of PdeWRKY6, and this regulation is partly or completely responsible for Pi uptake under low Pi availability. However, root and shoot Pi concentrations were lower in PdeWRKY6 RE transgenic lines compared to WT lines under low Pi availability (Figure 7e,f), while this was not found to be the case in PdePHT1;9 RE lines (Figure 5e,f,k,l). These data suggest that PdePHT1;9 might not be the only downstream

target of PdeWRKY6. In Arabidopsis, WRKY6 and WRKY42 are involved in the response to low Pi availability by regulating PHO1 expression (Chen et al., 2009). PHO1 is involved in the loading of Pi into the xylem of roots (Wang et al., 2004). Additionally, WRKY42 was shown to regulate Pi translocation and acquisition by controlling the expression of AtPHT1;1 (Su et al., 2015). Our phylogenetic analysis of PdeWRKY6 and its similar orthologs in Arabidopsis show that PdeWRKY6 is most closely related to AtWRKY42, AtWRKY31, and AtWRKY6. Thus, all previous studies and our data suggest that PdeWRKY6 may also regulate Pi uptake in poplar.

EXPERIMENTAL PROCEDURES

Plant materials and growth conditions

The poplar line NL895 (*P. deltoides* × *P. euramericana*) was used as plant material in this study. This poplar line was also used in our previous studies (Xiao et al., 2020a; Zhang et al., 2020a; Zhang et al., 2022). Therefore, genes identified in NL895 were given the suffix 'Pde'. Arabidopsis ecotype Columbia-0 (Col-0) and tobacco (*Nicotiana benthamiana*) were also used as plant materials.

The tissue culture of NL895 was conducted in WPM (Mccown & Lloyd, 1981) and the growth conditions were set as a 16/8 h light/dark photoperiod, a temperature of 28°C, and a light intensity of 100 μmol m−2 sec−1. The conditions for plants grown in soil (sand:peat, 50:50, v/v) were set as a 16/8 h light/dark photoperiod, a temperature of 25°C, and a light intensity of 100 μmol m−2 sec−1. For low Pi treatment in WPM, only 10% KH2PO4 was added to the nutrients of WPM (the final Pi concentration in the medium was 0.125 mm). The potassium level was restored by adding an additional 0.098 g L−1 K2SO4. For low Pi treatment in soil (only sand), a similar strategy was applied for the preparation of Hoagland's solution. The plants were grown in sand and irrigated with Hoagland's solution with 10% KH2PO4 (the final Pi in the solution was 0.050 mm).

RNA isolation, cDNA synthesis, and qRT-PCR

Total RNA was isolated and cDNA was synthesized according to our previous studies (Zhang et al., 2020a, Zhang et al., 2022). Briefly, RNA from different organs and tissues was isolated by an RNAprep Pure Kit (Cat No., DP432) according to the manufacturer's protocol (TIANGEN Biotech (Beijing) Co. Ltd., Beijing, China). cDNA was synthesized using First Strand cDNA Synthesis SuperMix for qPCR (Yisheng Co. Ltd., Shanghai, China). qRT-PCR was conducted using a Roche LightCycler 96 platform, and all reactions were performed with three biological and technical replicates. Primers used for qRT-PCR are listed in Table S1. Their specificity was confirmed by Sanger sequencing and melting curve analysis. Two genes, ACTIN and UBIQUITIN, were used as internal references for the calculation of the relative expression with the $2^{-\Delta\Delta Ct}$ method (Livak & Schmittgen, 2001).

Generation of transgenic poplar and Arabidopsis

All vectors used in this study were prepared in our laboratory and used in our previous studies (Xiao et al., 2020b; Zhang et al., 2020b; Zhang et al., 2022). The 2301S vector harbors a 2×35S promoter upstream of the multiple cloning site (MCS) which enables the constitutive expression of the downstream gene. A 35S::GUS unit was also included in this vector as a means of positive selection of transgenic lines. The complete coding sequences (CDSs) of target genes were cloned into the 2301S vector with a Gateway strategy.

The PHGRV vector was used to reduce expression of target genes. Two identical fragments of the CDS of the target gene were introduced into the PHGRV vector in opposite directions with BP Clonase (Gateway® BP Clonase TM II, Invitrogen, USA) to induce RNA interference. The GUS-encoding gene and the promoter of the target gene were cloned into the MCS of the pKGWFS7 vector to create a promoter–GUS fusion unit.

The successfully generated vectors were confirmed by PCR and Sanger sequencing and then introduced into Agrobacterium tumefaciens strain GV3101. Poplar line NL895 and Arabidopsis Col-0 were transformed according to methods described in our previous studies (Xiao et al., 2020a; Zhang et al., 2022). The resulting transgenic plants were confirmed by PCR-based DNA amplification, qRT-PCR-based expression assays, and GUS staining. GUS staining was performed according to a previously reported procedure (Lee & Schoffl, 1995). Confirmed transgenic lines were multiplied and propagated in WPM for further analyses. The transformation and screening of Arabidopsis transgenic lines were conducted according to our previous study (Zhang et al., 2020a). T3 lines with a single introduced copy were screened, and successful transformation of the target gene in these lines was confirmed by PCR and RT-PCR.

Measurement of tissue Pi concentrations

The measurement of Pi concentrations in shoot and root followed previous studies (Ames, 1966; Chiou et al., 2006). Briefly, fresh shoots and roots of Arabidopsis or poplar were used. All roots were first washed with deionized distilled water and cleaned with filter paper. The clean tissues were then grounded into powder in liquid nitrogen and these samples were transferred to Pi extraction buffer (10 mm Tris, 1 mm EDTA, 100 mm NaCl, 1 mm β-mercaptoethanol, and 1 mm phenylmethylsulfonyl fluoride, pH 8.0) at a ratio of 1 mg of sample (fresh weight) to 10 µl of extraction buffer. Then 1% glacial acetic acid was added to the reaction, followed by at 42°C for 30 min and centrifugation at 13 000 g for 5 min. Finally, 150 µl of the supernatant was added to a new reaction that contained 350 µl of assay buffer (0.35% NH_4MoO_4, 0.86 N H_2SO_4, and 1.4% ascorbic acid). The final reaction was incubated at 42°C for 30 min and absorbance was measured at 820 nm. Pi content was calculated according to a standard curve.

Yeast one-hybrid assay

The Y1H assay was performed according to the manufacturer's protocol (Clontech,

Shanghai, China). Briefly, the approximately 1.5-kb promoter sequence of PdePHT1;9 or a W-Box was cloned into pAbAi to create a bait vector. Full CDSs of PdeWRKY6 and PdeWRKY65 were cloned into pGADT7 to create two prey vectors. The bait vector was first transformed into yeast strain Y1HGold and employed to screen a proper concentration of aureobasidin A (AbA) in SD medium lacking Leu. Then, the prey vector was transformed into Y1HGold that had already been transformed with the bait vector. The interaction between prey and bait was examined in SD medium lacking Leu and containing a proper concentration of AbA.

Transient co-expression in tobacco

Co-expression of TF and the promoter of the target gene was conducted according to our previous studies (Zhang et al., 2020a; Zhang et al., 2022). Briefly, the full CDS of a gene encoding a TF was cloned into the pGreenII 62-SK vector to create an effector. The promoter of the target gene was cloned into the pGreenII 0800-LUC vector to create a reporter. Co-expression of the effector and reporter was achieved in tobacco leaves with an A. tumefaciens-based transient transformation procedure. Co-expression of empty pGreenII 62-SK vector and reporter was used as a control. The Dual-Luciferase® Reporter Assay System (Promega, USA) was used to measure the activity of renilla and firefly luciferase. Similarly, the full CDS of a gene encoding a TF was cloned into the DX218 vector to create the effector and the promoter of the target gene was cloned into the pKGWFS7 vector to create the reporter with GUS. The effector and reporter were co-expressed in tobacco leaves and co-expression of empty DX218 vector and reporter was considered as control. The transiently co-transformed tobacco leaves were stained with GUS staining buffer.

Subcellular location

The full CDS of PdeWRKY6 without stop codon was cloned into the 35SGFP vector to create 35S::WRKY6:GFP, expressing a PdeWRKY6-GFP fusion protein. Transient transformation of this vector into 6-week-old tobacco leaves was conducted and the

transformed leaves were observed with a fluorescence microscope (Leica, DM2500, Shanghai, China).

Electrophoretic mobility shift assay

The full CDS of PdeWRKY65 or PdeWRKY6 without stop codon was cloned into the pHMGWA vector to express a 6×His:MBP:WRKY6:6×His fusion protein in Escherichia coli strain Rosetta (DE3) with an induction condition of 18°C and 0.3 mm isopropyl β-d-1-thiogalactopyranoside for 25 h. The fused proteins were purified with the Ni Sepharose 6 Fast Flow Kit (GE Healthcare, Shanghai, China). Meanwhile, a probe with sequence 'TTTGACTGTTTGACTCGTTGACTG' was synthesized and labeled with biotin at the 3′-hydroxyl end of the sense strand (the core bases of W-Boxes are underlined). The mutated probe (mProbe) 'TTCCCCTGTTGGGGTCGTAAAATG' was also synthesized and labeled (core bases of the W-Boxes were substituted). An unlabeled probe was also synthesized and used as the competitor. The purified fusion protein and probe, mProbe, and competitor were mixed in different ratios, subjected to electrophoresis on a 6.0% polyacrylamide gel, and then transferred to a nylon membrane. The membrane was then scanned using a CCD imaging device (Molecular Imager ChemiDoc XRS+).

ChIP-qPCR

The ChIP-qPCR experiment was performed according to previous studies (Xu et al., 2021; Zhang, Qi, et al., 2016). The 2×35S::WRKY65:Flag, 2×35S::WRKY6:Flag, and 2×35S::Flag vectors were generated, and these vectors were used to transform poplar NL895 with Agrobacterium rhizogenes strain K599. This enabled the creation of transformed hairy roots. The fresh hairy roots from 10–20 explants were collected and crosslinked with 1% formaldehyde. The chromatin was extracted and an anti-Flag antibody was used to immunoprecipitate the protein–DNA complex. Primer pairs covering the W-Box motifs in the promoter of PdePHT1;9 were designed and a primer pair not covering the W-Box motif in the promoter was used as control. The precipitated

DNA was used as a template to conduct the qPCR assay. The precipitated DNA from hairy roots transformed with 2×35S::Flag was used as control and its DNA concentration was used for normalization. At least three biological replicates were included for each DNA–protein interaction.

Yeast two-hybrid assay

The Y2H assay was performed according to the manufacturer's protocol (Clontech, Shanghai, CN). Briefly, the full CDSs of PdeWRKY6 and PdeWRKY65 were cloned into the pGBKT7 and pGADT7 vectors, respectively. The two vectors were successively transformed into yeast strain Y2HGold. The successful transformants were screened and confirmed in SD/−Trp/−Leu medium and the interaction was examined in SD/−Trp/−Leu/−His/−Ade medium with X-α-Gal and 100 ng ml−1 AbA. Yeast transformed with pGBKT7-Lam and pGADT7-T was considered as a negative control, while yeast transformed with pGBKT7-53 and pGADT7-T was considered as a positive control.

Bioinformatics and statistical analysis

Whole plants including roots, leaves, young stems, and shoots from three PdeWRKY65 OE lines were collected and mixed to prepare three transgenic biological samples (at least five plants were collected for each transgenic line), while a similar strategy was used to prepare the three WT biological samples used as plant material. The RNA-Seq data were deposited in the NCBI Sequence Read Archive database under accession No. PRJNA852675. For RNA-Seq analysis, RNA samples that met the quality requirements were sequenced with a NovaSeq Sequencing System. Raw reads were filtered by using Trimmomatic software with default parameter settings (Bolger et al., 2014). Clean reads were mapped onto the reference genome of P. trichocarpa version 3.0 (Tuskan et al., 2006) and read counts for each sample were calculated by using the software hisat2 and featureCounts (Kim et al., 2019; Liao et al., 2014), respectively. Differentially expressed genes between WT and each transgenic line were identified by

using DESeq2 software (Love et al., 2014). Three biological replicates were included for each plant line. The phylogenetic trees were constructed by using Mega X software with a neighbor-joining method (Kumar et al., 2018). Statistical analysis was performed by using R software (https://www.r-project.org/). The functions 'aov' and 'Tukey HSD' implemented in R software were used for analysis of variance and multiple comparisons, respectively.

Data availability

The data was deposited on NCBI Sequence Read Archive database under accession No. PRJNA852675. All other data supporting the findings of this study are available within the paper and within its supplementary data published online.

ACKNOWLEDGMENTS

Financial support for this work was provided by the National Natural Science Foundation of China (NSFC accession No. 32171745).

AUTHOR CONTRIBUTIONS

YX, TN, ZY, HL, CG, DY, RW, and WN conducted the experiments. WN organized and supervised the whole project. TN, HJ, SL, JPH, and WN performed data analysis and wrote the manuscript. HJ, SL, JPH, and WN edited the manuscript.

CONFLICT OF INTEREST

The authors declare that they have no conflict of interest.

FIGURE LEGENDS

Fig. 1. Growth and development in over expression (OE) *PdeWRKY65* poplar transgenic lines grown in soil with normal phosphate (Pi) availability.
(a). The above-ground performance of OE *PdeWRKY65* transgenic lines grown in soil with the normal Pi availability. All plants were grown in soil for 100 d. (b). Roots of the plant in Fig. 1a. (c) Plant height, (d) the 6th internode (from shoots) diameter, (e) root Pi concentration, and (f) shoot Pi concentration of OE *PdeWRKY65* transgenic

lines grown in soil for 100. Bars represent means ± SEM (n=30). Different letters above bars indicate significant differences in multiple comparisons based on Tukey method under P values < 0.05.

Fig. 2. Root and shoot Pi concentrations in reduced expression (RE) *PdeWRKY65* transgenic lines and the expression of *PdeWRKY65* after 10 d growth at low Pi availability

(a). Root Pi concentrations in RE *PdeWRKY65* transgenic lines. (b). Shoot Pi concentrations in RE *PdeWRKY65* transgenic lines. (c). Relative expression of *PdeWRKY65* after 10 d growth at low Pi availability (0.125 mM P). The expression of *PdeWRKY65* under normal Pi availability (1.25 mM P) was set as 1-fold. Bars represent means ± SEM (n=30). Different letters above bars indicate significant differences in multiple comparisons based on Tukey method under P values < 0.05.

Fig. 3. The expression of *PdePHT1;9* is increased under low phosphate (Pi) availability.

(a). Phylogenic tree of PdePHT1;9 and its closest orthologs in Arabidopsis, generated using Mega X. (b). Relative expression of *PdePHT1;9* after 10 d growth at low Pi availability (0.125 mM P). The expression of *PdePHT1;9* under normal Pi availability (1.25 mM P) was set as 1-fold. (c). The relative expression of *PdePHT1;9* in different tissues. (d). The relative expression of *PdePHT1;9* in WT and OE/RE *PdeWRKY65* transgenic lines. The whole tissue culture plants were used as plant materials. The expression of *PdePHT1;9* in WT was set as 1-fold. (e). GUS staining analysis of the expression of *PdePHT1;9*. A schematic diagram for the construction of the *PdePHT1;9::GUS* vector was shown in the top left. The staining of *PdePHT1;9::GUS* transgenic line under normal and low Pi availabilities are shown in left and right, respectively.

Fig. 4. Confirmation that PdeWRKY65 negatively regulates *PdePHT1;9* expression by binding to a W-Box in the promotor of *PdePHT1;9*

(a). Y1H confirmation of the binding of *PdePHT1;9* promoter by PdeWRKY65. (b). Co-expression of *PdePHT1;9::GUS* and *35S*::*PdeWRKY65* in tobacco leaves. (c). Dual luciferase assay of the prohibition of *PdePHT1;9* expression by PdeWRKY65. (d). EMSA confirmation of the binding of W-Box in *PdePHT1;9* promoter by PdeWRKY65. (e). ChIP-qPCR assay of the binding of *PdePHT1;9* promoter by PdeWRKY65. Fragment of F1 does not harbor a W-Box, while F2 to F4 harbor W-Boxes at -916, -528 and -246 bp, respectively. The DNA abundance of *35S*::*Flag* was set as 1-fold. Different letters above bars indicate significant differences in T test.

Fig. 5. Root and shoot Pi concentrations in over (OE) and reduced (RE) expression *PdePHT1;9* transgenic lines grown under low Pi availability

Growth and development of OE and RE *PdePHT1;9* transgenic lines grown in WPM with normal Pi availability (1.25 mM P) (a and d) and low Pi availability (0.125 mM P) (g and j) for 15 days. Root and shoot Pi concentrations in OE *PdeWRKY65* transgenic lines (b and c) and Root and shoot Pi concentrations in RE *PdeWRKY65* transgenic lines (e and f) grown in WPM with normal Pi availability (1.25 mM P). Root and shoot Pi concentrations in OE *PdeWRKY65* transgenic lines (h and i) and Root and shoot Pi concentrations in RE *PdeWRKY65* transgenic lines (k and l) grown in WPM with low Pi availability (0.125 mM P).<="" span="" style="font-family: "Times New Roman"; font-size: 12pt;">Bars represent means ± SEM (n=30). Different letters above bars indicate significant differences in multiple comparisons based on Tukey method under P values < 0.05.

Fig. 6. Confirmation that PdeWRKY6 positively regulates *PdePHT1;9* expression by binding to a W-Box in the promotor of *PdePHT1;9*

(a). Phylogenic tree of PdeWRKY6 and its closest orthologs in Arabidopsis created using Mega X. (b). Subcellular location of PdeWRKY6. PdeWRKY6 was fused with GFP and RFP indicates a nucleus marker. (c). Relative expression of *PdeWRKY6* in WT and OE/RE *PdeWRKY65* transgenic lines. The whole tissue culture plants were used as plant materials. The expression of *PdeWRKY6* in WT was set as 1-fold. (d). Relative expression of *Pde WRKY6* in different tissues. The expression of *Pde*

WRKY6 in root was set as 1-fold. (e). The relative expression of *Pde RKY6* after 10 d growth at low Pi availability (0.125 mM P). The expression of *PdePHT1;9* under normal Pi availability (1.25 mM P) was set as 1-fold. (f). The relative expression of *PdePHT1;9* in WT and OE/RE *PdeWRKY6* transgenic lines. The whole tissue culture plants were used as plant materials. The expression of *PdePHT1;9* in WT was set as 1-fold. (g). Y1H confirmation of the binding of *PdePHT1;9* promoter by PdeWRKY6. (h). Co-expression of *PdePHT1;9::GUS* and *35S*::*PdeWRKY65* in tobacco leaves. (i). Dual luciferase assay of the prohibition of *PdePHT1;9* expression by PdeWRKY6. (j). ChIP-qPCR assay of the binding of *PdePHT1;9* promoter by PdeWRKY6. The DNA abundance of *35S*::*Flag* was set as 1-fold. The primer design for this analysis is identical to Fig. 5i. (k). EMSA confirmation of the binding of W-Box in *PdePHT1;9* promoter by PdeWRKY6. Different letters above bars indicate significant differences in T test.

Fig. 7. Root and shoot Pi concentrations in over (OE) and reduced (RE) expression *PdeWRKY6* transgenic lines under low Pi availability

(a). Growth and development of (a) OE *PdeWRKY6* transgenic lines and (d) RE *PdeWRKY6* transgenic lines grown in WPM with low Pi availability (0.125 mM P) for 15 days. Root (b) and shoot (c) Pi concentrations in OE *PdeWRKY6* transgenic lines grown on WPM with low Pi availability. Root (e) and shoot (f) Pi concentrations in RE *PdeWRKY6* transgenic lines grown on WPM with low Pi availability. Bars represent means ± SEM (n=30). Different letters above bars indicate significant differences in multiple comparisons based on Tukey method under P values < 0.05.

Fig. 8. A regulatory model for *PdeWRKY65, PdeWRKY6, PdePHT1;9* regulating tissue Pi concentration in poplar

In this model, under normal Pi availability, a homeostasis regulation of *PdePHT1;9* by PdeWRKY6 and PdeWRKY65. This homeostasis regulation enables poplar to translocate a proper amount of Pi to shoots. Under normal Pi availability, the expression *PdeWRKY65* is decreased and the expression of *PdeWRKY6* increased in response to low Pi condition. PdeWRKY65 inhibits the expression of *PdePHT1;9*,

while PdeWRKY6 activates the expression of *PdePHT1;9* by binding to the W-Box in the promotor of *PdePHT1;9*. Therefore, the expression of *PdePHT1;9* is increased by dual regulation. The increased expression of *PdePHT1;9* results in more Pi translocated to shoots in poplar under low Pi availability.

REFERENCES

Ames, B.N. (1966) Assay of inorganic phosphate, total phosphate and phosphatase. *Methods in Enzymology*, **8**, 115-118.

Bieleski, R.L. (1973) Phosphate Pools, Phosphate Transport, and Phosphate Availability. *Annu Rev Plant Phys*, **24**, 225-252.

Bolger, A.M., Lohse, M. and Usadel, B. (2014) Trimmomatic: a flexible trimmer for Illumina sequence data. *Bioinformatics*, **30**, 2114-2120.

Bucher, M. (2007) Functional biology of plant phosphate uptake at root and mycorrhiza interfaces. *New Phytol*, **173**, 11-26.

Chen, A., Chen, X., Wang, H., Liao, D., Gu, M., Qu, H., Sun, S. and Xu, G. (2014) Genome-wide investigation and expression analysis suggest diverse roles and genetic redundancy of Pht1 family genes in response to Pi deficiency in tomato. *BMC Plant Biol*, **14**, 61.

Chen, Y.F., Li, L.Q., Xu, Q., Kong, Y.H., Wang, H. and Wu, W.H. (2009) The WRKY6 Transcription Factor Modulates PHOSPHATE1 Expression in Response to Low Pi Stress in Arabidopsis. *Plant Cell*, **21**, 3554-3566.

Chiou, T.J., Aung, K., Lin, S.I., Wu, C.C., Chiang, S.F. and Su, C.L. (2006) Regulation of phosphate homeostasis by MicroRNA in Arabidopsis. *Plant Cell*, **18**, 412-421.

Dai, X.Y., Wang, Y.Y. and Zhang, W.H. (2016) OsWRKY74, a WRKY transcription factor, modulates tolerance to phosphate starvation in rice. *Journal of Experimental Botany*, **67**, 947-960.

Devaiah, B.N., Karthikeyan, A.S. and Raghothama, K.G. (2007) WRKY75 transcription factor is a modulator of phosphate acquisition and root development in arabidopsis. *Plant Physiol*, **143**, 1789-1801.

Gu, M.A., Chen, A.Q., Sun, S.B. and Xu, G.H. (2016) Complex Regulation of Plant

802 Phosphate Transporters and the Gap between Molecular Mechanisms and
803 Practical Application: What Is Missing? *Mol Plant*, **9**, 396-416.
804 **Guo, Y., Ren, G., Zhang, K., Li, Z., Miao, Y. and Guo, H.** (2021) Leaf senescence:
805 progression, regulation, and application. *Molecular Horticulture*, **1**, 5.
806 **Hamburger, D., Rezzonico, E., Petetot, J.M.C., Somerville, C. and Poirier, Y.** (2002)
807 Identification and characterization of the Arabidopsis PHO1 gene involved in
808 phosphate loading to the xylem. *Plant Cell*, **14**, 889-902.
809 **Jia, H.F., Ren, H.Y., Gu, M., Zhao, J.N., Sun, S.B., Zhang, X., Chen, J.Y., Wu, P.**
810 **and Xu, G.H.** (2011) The Phosphate Transporter Gene OsPht1;8 Is Involved in
811 Phosphate Homeostasis in Rice. *Plant Physiol*, **156**, 1164-1175.
812 **Kim, D., Paggi, J.M., Park, C., Bennett, C. and Salzberg, S.L.** (2019) Graph-based
813 genome alignment and genotyping with HISAT2 and HISAT-genotype. *Nat*
814 *Biotechnol*, **37**, 907-915.
815 **Kumar, S., Stecher, G., Li, M., Knyaz, C. and Tamura, K.** (2018) MEGA X:
816 Molecular Evolutionary Genetics Analysis across Computing Platforms.
817 *Molecular Biology and Evolution*, **35**, 1547-1549.
818 **Lapis-Gaza, H.R., Jost, R. and Finnegan, P.M.** (2014) Arabidopsis PHOSPHATE
819 TRANSPORTER1 genes PHT1;8 and PHT1;9 are involved in root-to-shoot
820 translocation of orthophosphate. *Bmc Plant Biology*, **14**.
821 **Lee, J.H. and Schoffl, F.** (1995) GUS activity staining in gels: A powerful tool for
822 studying protein interactions in plants. *Plant Mol Biol Rep*, **13**, 346-354.
823 **Liao, Y., Smyth, G.K. and Shi, W.** (2014) featureCounts: an efficient general purpose
824 program for assigning sequence reads to genomic features. *Bioinformatics*, **30**,
825 923-930.
826 **Livak, K.J. and Schmittgen, T.D.** (2001) Analysis of relative gene expression data
827 using real-time quantitative PCR and the 2(T)(-Delta Delta C) method. *Methods*,
828 **25**, 402-408.
829 **Lopez-Arredondo, D.L., Leyva-Gonzalez, M.A., Gonzalez-Morales, S.I., Lopez-**
830 **Bucio, J. and Herrera-Estrella, L.** (2014) Phosphate Nutrition: Improving
831 Low-Phosphate Tolerance in Crops. *Annu Rev Plant Biol*, **65**, 95-123.
832 **Love, M.I., Huber, W. and Anders, S.** (2014) Moderated estimation of fold change

and dispersion for RNA-seq data with DESeq2. *Genome Biol*, **15**, 550.

Ma, B., Zhang, L., Gao, Q., Wang, J., Li, X., Wang, H., Liu, Y., Lin, H., Liu, J., Wang, X., Li, Q., Deng, Y., Tang, W., Luan, S. and He, Z. (2021) A plasma membrane transporter coordinates phosphate reallocation and grain filling in cereals. *Nat Genet*, **53**, 906-915.

Mccown, B.H. and Lloyd, G. (1981) Woody Plant Medium (Wpm) - a Mineral Nutrient Formulation for Microculture of Woody Plant-Species. *Hortscience*, **16**, 453-453.

Misson, J., Raghothama, K.G., Jain, A., Jouhet, J., Block, M.A., Bligny, R., Ortet, P., Creff, A., Somerville, S., Rolland, N., Doumas, P., Nacry, P., Herrerra-Estrella, L., Nussaume, L. and Thibaud, M.C. (2005) A genome-wide transcriptional analysis using Arabidopsis thaliana Affymetrix gene chips determined plant responses to phosphate deprivation. *P Natl Acad Sci USA*, **102**, 11934-11939.

Mudge, S.R., Rae, A.L., Diatloff, E. and Smith, F.W. (2002a) Expression analysis suggests novel roles for members of the Pht1 family of phosphate transporters in Arabidopsis. *Plant J*, **31**, 341-353.

Mudge, S.R., Rae, A.L., Diatloff, E. and Smith, F.W. (2002b) Expression analysis suggests novel roles for members of the Pht1 family of phosphate transporters in Arabidopsis. *Plant J*, **31**, 341-353.

Nagarajan, V.K., Jain, A., Poling, M.D., Lewis, A.J., Raghothama, K.G. and Smith, A.P. (2011) Arabidopsis Pht1;5 Mobilizes Phosphate between Source and Sink Organs and Influences the Interaction between Phosphate Homeostasis and Ethylene Signaling. *Plant Physiol*, **156**, 1149-1163.

Raghothama, K.G. (1999) Phosphate Acquisition. *Annu Rev Plant Physiol Plant Mol Biol*, **50**, 665-693.

Remy, E., Cabrito, T.R., Batista, R.A., Teixeira, M.C., Sa-Correia, I. and Duque, P. (2012) The Pht1;9 and Pht1;8 transporters mediate inorganic phosphate acquisition by the Arabidopsis thaliana root during phosphorus starvation. *New Phytol*, **195**, 356-371.

Ren, F., Zhao, C.Z., Liu, C.S., Huang, K.L., Guo, Q.Q., Chang, L.L., Xiong, H. and

Li, X.B. (2014) A Brassica napus PHT1 phosphate transporter, BnPht1;4, promotes phosphate uptake and affects roots architecture of transgenic Arabidopsis. *Plant Molecular Biology*, **86**, 595-607.

Shen, J., Yuan, L., Zhang, J., Li, H., Bai, Z., Chen, X., Zhang, W. and Zhang, F. (2011) Phosphorus dynamics: from soil to plant. *Plant Physiol*, **156**, 997-1005.

Stigter, K.A. and Plaxton, W.C. (2015) Molecular Mechanisms of Phosphorus Metabolism and Transport during Leaf Senescence. *Plants (Basel)*, **4**, 773-798.

Su, T., Xu, Q., Zhang, F.C., Chen, Y., Li, L.Q., Wu, W.H. and Chen, Y.F. (2015) WRKY42 Modulates Phosphate Homeostasis through Regulating Phosphate Translocation and Acquisition in Arabidopsis. *Plant Physiol*, **167**, 1579-U1717.

Sun, S., Gu, M., Cao, Y., Huang, X., Zhang, X., Ai, P., Zhao, J., Fan, X. and Xu, G. (2012) A constitutive expressed phosphate transporter, OsPht1;1, modulates phosphate uptake and translocation in phosphate-replete rice. *Plant Physiol*, **159**, 1571-1581.

Sun, T., Li, M., Shao, Y., Yu, L. and Ma, F. (2017) Comprehensive Genomic Identification and Expression Analysis of the Phosphate Transporter (PHT) Gene Family in Apple. *Front Plant Sci*, **8**, 426.

Tsuda, K., Mine, A., Bethke, G., Igarashi, D., Botanga, C.J., Tsuda, Y., Glazebrook, J., Sato, M. and Katagiri, F. (2013) Dual Regulation of Gene Expression Mediated by Extended MAPK Activation and Salicylic Acid Contributes to Robust Innate Immunity in Arabidopsis thaliana. *Plos Genet*, **9**.

Tuskan, G.A., DiFazio, S., Jansson, S., Bohlmann, J., Grigoriev, I., Hellsten, U., Putnam, N., Ralph, S., Rombauts, S., Salamov, A., Schein, J., Sterck, L., Aerts, A., Bhalerao, R.R., Bhalerao, R.P., Blaudez, D., Boerjan, W., Brun, A., Brunner, A., Busov, V., Campbell, M., Carlson, J., Chalot, M., Chapman, J., Chen, G.L., Cooper, D., Coutinho, P.M., Couturier, J., Covert, S., Cronk, Q., Cunningham, R., Davis, J., Degroeve, S., Dejardin, A., Depamphilis, C., Detter, J., Dirks, B., Dubchak, I., Duplessis, S., Ehlting, J., Ellis, B., Gendler, K., Goodstein, D., Gribskov, M., Grimwood, J., Groover, A., Gunter, L., Hamberger, B., Heinze, B., Helariutta, Y., Henrissat, B., Holligan, D., Holt, R., Huang, W., Islam-Faridi, N., Jones, S., Jones-Rhoades, M., Jorgensen,

R., Joshi, C., Kangasjarvi, J., Karlsson, J., Kelleher, C., Kirkpatrick, R., Kirst, M., Kohler, A., Kalluri, U., Larimer, F., Leebens-Mack, J., Leple, J.C., Locascio, P., Lou, Y., Lucas, S., Martin, F., Montanini, B., Napoli, C., Nelson, D.R., Nelson, C., Nieminen, K., Nilsson, O., Pereda, V., Peter, G., Philippe, R., Pilate, G., Poliakov, A., Razumovskaya, J., Richardson, P., Rinaldi, C., Ritland, K., Rouze, P., Ryaboy, D., Schmutz, J., Schrader, J., Segerman, B., Shin, H., Siddiqui, A., Sterky, F., Terry, A., Tsai, C.J., Uberbacher, E., Unneberg, P., Vahala, J., Wall, K., Wessler, S., Yang, G., Yin, T., Douglas, C., Marra, M., Sandberg, G., Van de Peer, Y. and Rokhsar, D. (2006) The genome of black cottonwood, Populus trichocarpa (Torr. & Gray). *Science*, **313**, 1596-1604.

Wang, H., Xu, Q., Kong, Y.H., Chen, Y., Duan, J.Y., Wu, W.H. and Chen, Y.F. (2014) Arabidopsis WRKY45 transcription factor activates PHOSPHATE TRANSPORTER1;1 expression in response to phosphate starvation. *Plant Physiol*, **164**, 2020-2029.

Wang, P.F., Li, G.Z., Li, G.W., Yuan, S.S., Wang, C.Y., Xie, Y.X., Guo, T.C., Kang, G.Z. and Wang, D.W. (2021) TaPHT1;9-4B and its transcriptional regulator TaMYB4-7D contribute to phosphate uptake and plant growth in bread wheat. *New Phytol*, **231**, 1968-1983.

Wang, Y., Ribot, C., Rezzonico, E. and Poirier, Y. (2004) Structure and expression profile of the Arabidopsis PHO1 gene family indicates a broad role in inorganic phosphate homeostasis. *Plant Physiol*, **135**, 400-411.

Xiao, Z., Zhang, Y., Liu, M., Zhan, C., Yang, X., Nvsvrot, T., Yan, Z. and Wang, N. (2020a) Coexpression analysis of a large-scale transcriptome identified a calmodulin-like protein regulating the development of adventitious roots in poplar. *Tree Physiol*, **40**, 1405-1419.

Xiao, Z.A., Zhang, Y., Liu, M.F., Zhan, C., Yang, X.Q., Nvsvrot, T., Yan, Z.G. and Wang, N. (2020b) Coexpression analysis of a large-scale transcriptome identified a calmodulin-like protein regulating the development of adventitious roots in poplar. *Tree Physiol*, **40**, 1405-1419.

Xu, H., Luo, D. and Zhang, F. (2021) DcWRKY75 promotes ethylene induced petal

926 senescence in carnation (Dianthus caryophyllus L.). *Plant J*, **108**, 1473-1492.
927 **Ye, Q., Wang, H., Su, T., Wu, W.H. and Chen, Y.F.** (2018) The Ubiquitin E3 Ligase
928 PRU1 Regulates WRKY6 Degradation to Modulate Phosphate Homeostasis in
929 Response to Low-Pi Stress in Arabidopsis. *Plant Cell*, **30**, 1062-1076.
930 **Zhang, C., Meng, S., Li, M. and Zhao, Z.** (2016a) Genomic Identification and
931 Expression Analysis of the Phosphate Transporter Gene Family in Poplar. *Front*
932 *Plant Sci*, **7**, 1398.
933 **Zhang, F., Qi, B., Wang, L.K., Zhao, B., Rode, S., Riggan, N.D., Ecker, J.R. and**
934 **Qiao, H.** (2016b) EIN2-dependent regulation of acetylation of histone H3K14
935 and non-canonical histone H3K23 in ethylene signalling. *Nat Commun*, **7**.
936 **Zhang, Y., Yang, X., Cao, P., Xiao, Z., Zhan, C., Liu, M., Nvsvrot, T. and Wang, N.**
937 (2020a) The bZIP53-IAA4 module inhibits adventitious root development in
938 Populus. *J Exp Bot*, **71**, 3485-3498.
939 **Zhang, Y., Yang, X., Nvsvrot, T., Huang, L., Cai, G., Ding, Y., Ren, W. and Wang,**
940 **N.** (2021) The transcription factor WRKY75 regulates the development of
941 adventitious roots, lateral buds and callus by modulating hydrogen peroxide
942 content in poplar. *Journal of Experimental Botany*.
943 **Zhang, Y., Yang, X.Q., Cao, P., Xiao, Z.A., Zhan, C., Liu, M.F., Nvsvrot, T. and**
944 **Wang, N.** (2020b) The bZIP53-IAA4 module inhibits adventitious root
945 development in Populus. *Journal of Experimental Botany*, **71**, 3485-3498.
946 **Zhang, Y., Yang, X.Q., Nvsvrot, T., Huang, L.Y., Cai, G.H., Ding, Y.W., Ren, W.Y.**
947 **and Wang, N.A.** (2022) The transcription factor WRKY75 regulates the
948 development of adventitious roots, lateral buds and callus by modulating
949 hydrogen peroxide content in poplar. *Journal of Experimental Botany*, **73**, 1483-
950 1498.
951
952
953
954
955
956 **Figure 1.**

957

958

959

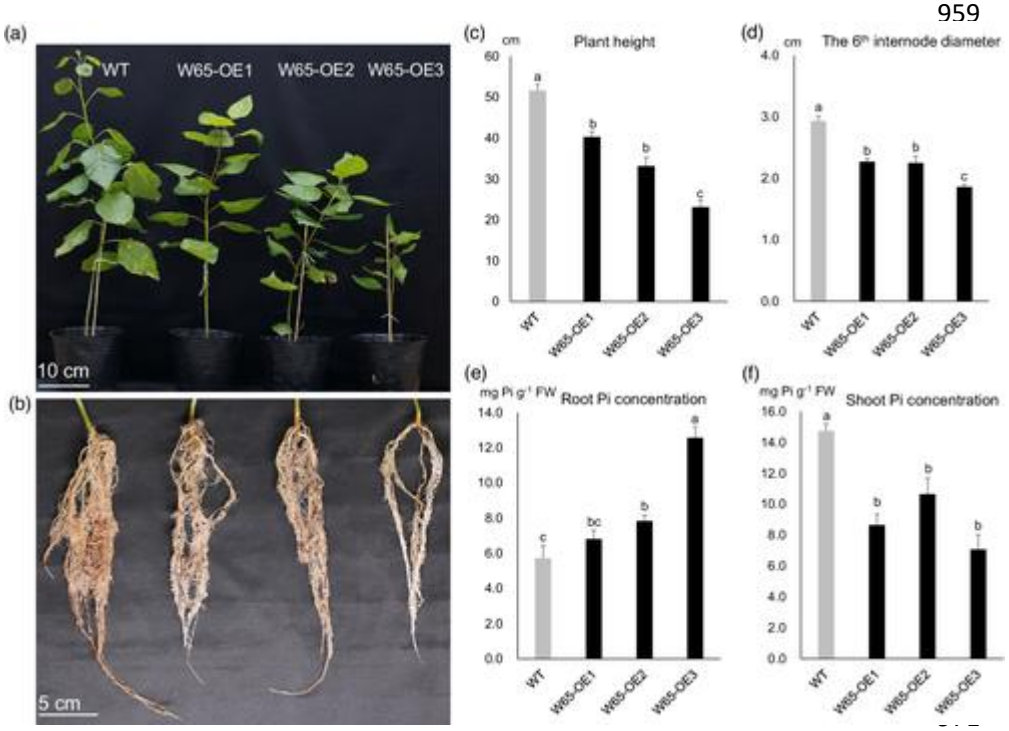

972

973

974 **Figure 2**

975

976

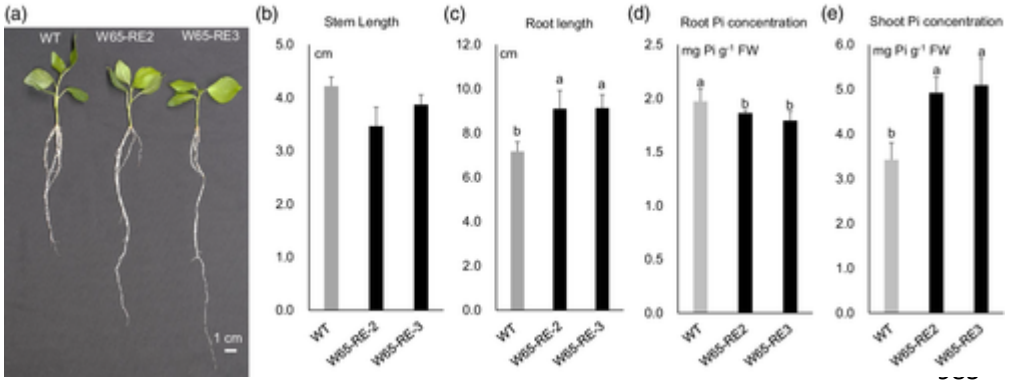

984

985

Figure 3

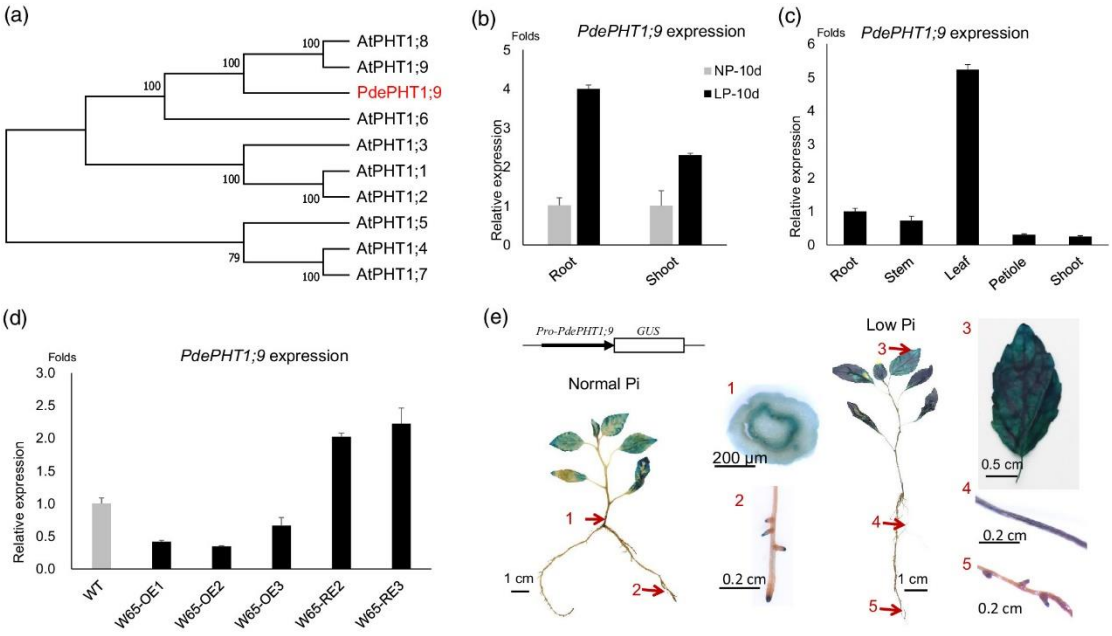
(a)
AtPHT1;8
AtPHT1;9
PdePHT1;9
AtPHT1;6
AtPHT1;3
AtPHT1;1
AtPHT1;2
AtPHT1;5
AtPHT1;4
AtPHT1;7
100
100
100
100
100
79
100
(b)
PdePHT1;9 expression
Folds
NP-10d
LP-10d
Relative expression
Root
Shoot
(c)
PdePHT1;9 expression
Folds
Relative expression
Root
Stem
Leaf
Petiole
Shoot
(d)
PdePHT1;9 expression
Folds
Relative expression
WT
W65-OE1
W65-OE2
W65-OE3
W65-RE2
W65-RE3
(e)
Pro-PdePHT1;9
GUS
Normal Pi
Low Pi
1 cm
200 μm
0.2 cm
0.5 cm
0.2 cm
1 cm
0.2 cm

Figure 4

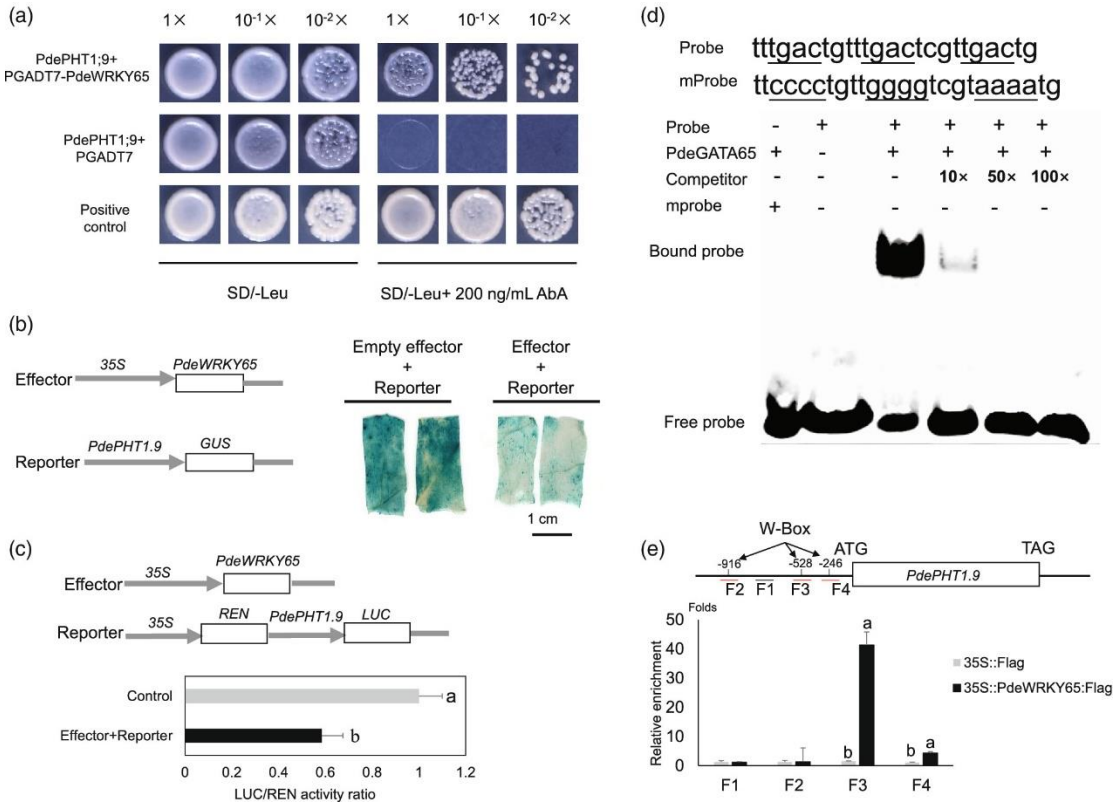
(a)
1×
10-1×
10-2×
1×
10-1×
10-2×
PdePHT1;9+ PGADT7-PdeWRKY65
PdePHT1;9+ PGADT7
Positive control
SD/-Leu
SD/-Leu+ 200 ng/mL AbA
(b)
Effector
35S
PdeWRKY65
Reporter
PdePHT1.9
GUS
Empty effector + Reporter
Effector + Reporter
1 cm
(c)
Effector
35S
PdeWRKY65
Reporter
35S
REN
PdePHT1.9
LUC
Control
Effector+Reporter
a
b
0
0.2
0.4
0.6
0.8
1
1.2
LUC/REN activity ratio
(d)
Probe
tttgactgtttgactcgttgactg
mProbe
ttcccctgttggggtcgtaaaatg
Probe
PdeGATA65
Competitor
mprobe
10×
50×
100×
Bound probe
Free probe
(e)
W-Box
ATG
TAG
-916
-528
-246
F2
F1
F3
F4
PdePHT1.9
Folds
50
40
30
20
10
0
Relative enrichment
a
b
b
a
35S::Flag
35S::PdeWRKY65:Flag
F1
F2
F3
F4

997 **Figure 5**

998

999

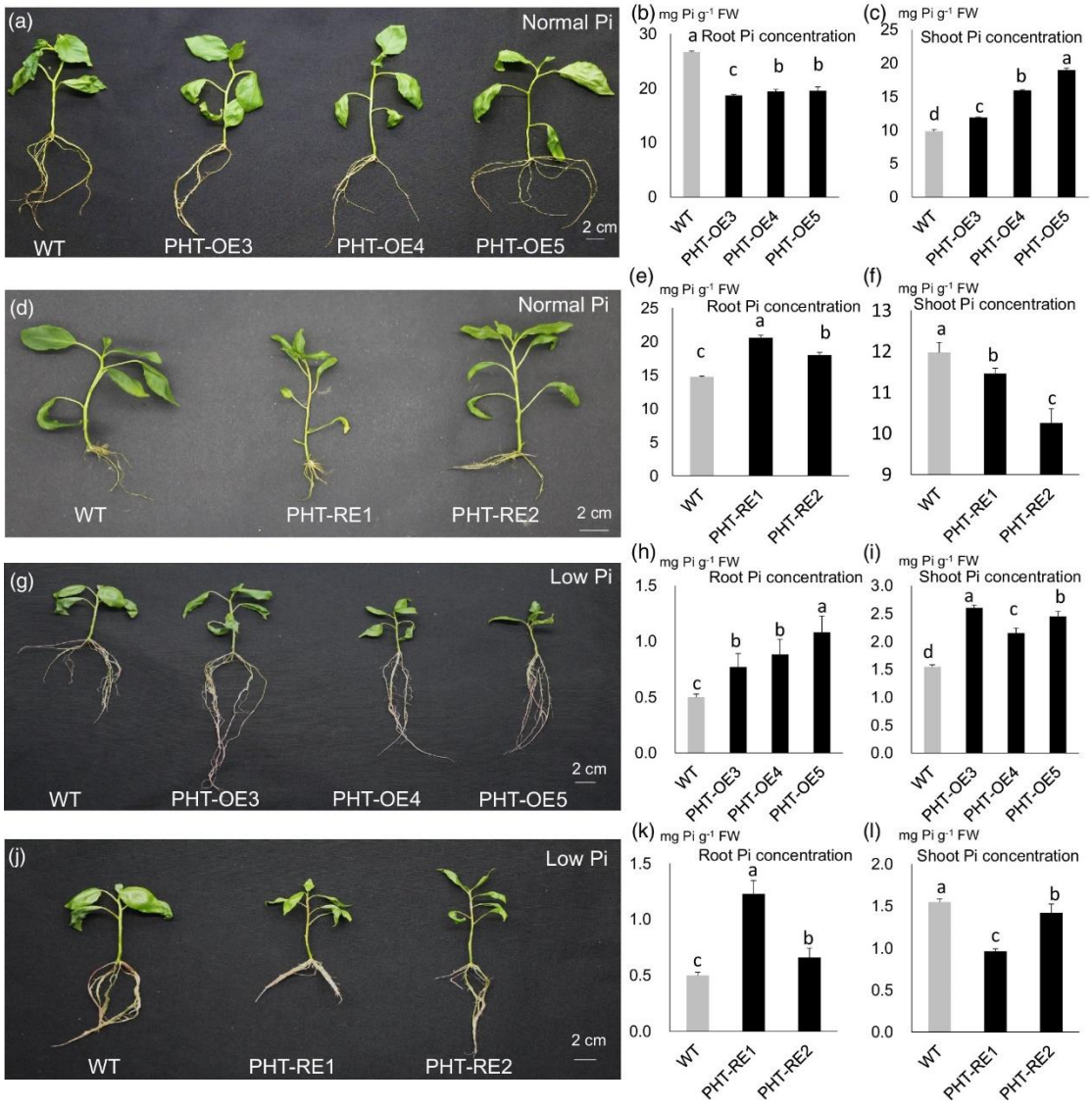

1000

1001

1002

Figure 6

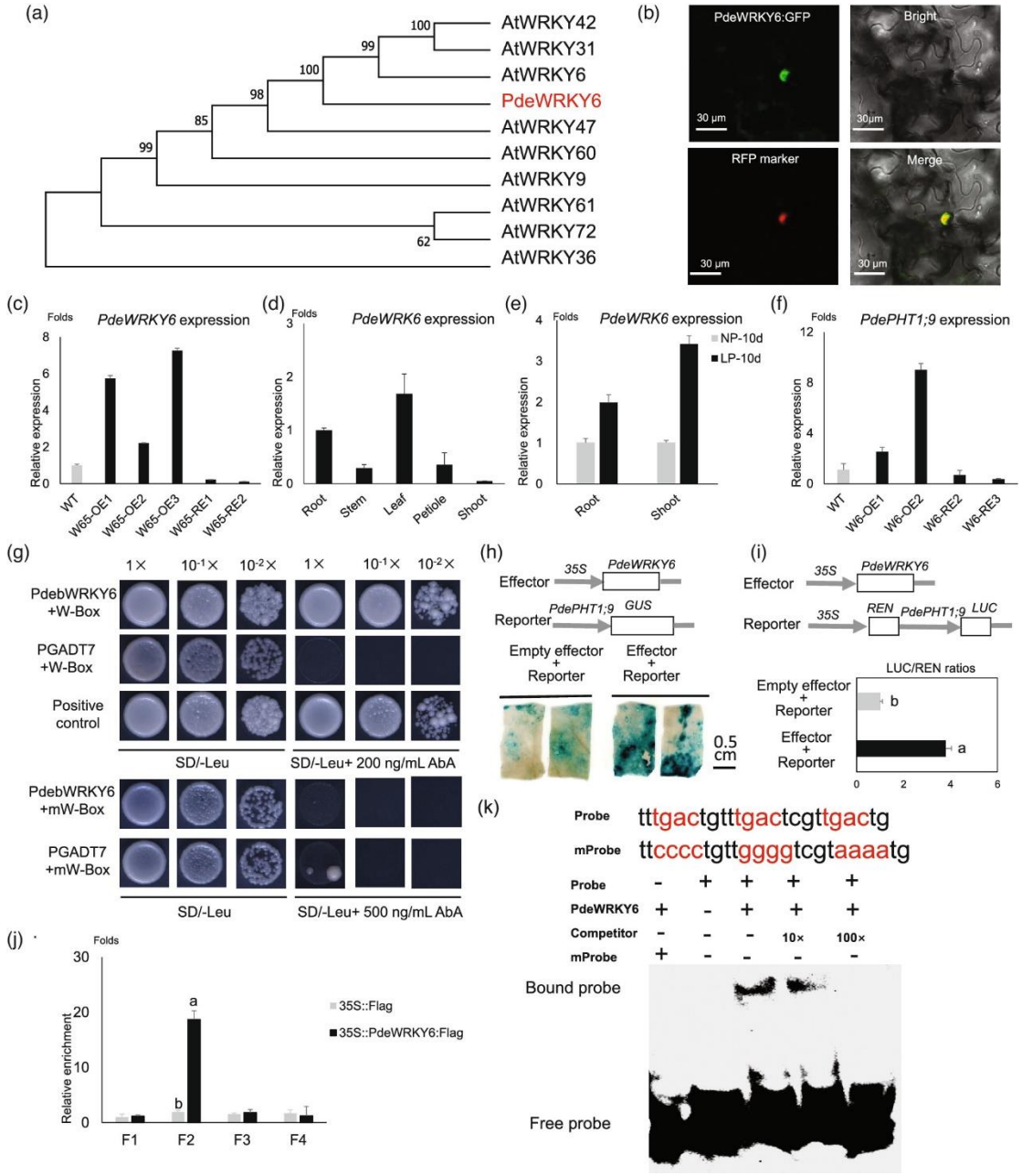
(a)
AtWRKY42
AtWRKY31
AtWRKY6
PdeWRKY6
AtWRKY47
AtWRKY60
AtWRKY9
AtWRKY61
AtWRKY72
AtWRKY36
(b)
PdeWRKY6:GFP
Bright
RFP marker
Merge
(c)
PdeWRKY6 expression
(d)
PdeWRK6 expression
(e)
PdeWRK6 expression
NP-10d
LP-10d
(f)
PdePHT1;9 expression
Relative expression
Folds
WT
W65-OE1
W65-OE2
W65-OE3
W65-RE1
W65-RE2
Root
Stem
Leaf
Petiole
Shoot
W6-OE1
W6-OE2
W6-RE2
W6-RE3
(g)
PdebWRKY6 +W-Box
PGADT7 +W-Box
Positive control
PdebWRKY6 +mW-Box
PGADT7 +mW-Box
SD/-Leu
SD/-Leu+ 200 ng/mL AbA
SD/-Leu+ 500 ng/mL AbA
(h)
Effector
Reporter
35S
PdeWRKY6
PdePHT1;9
GUS
Empty effector + Reporter
Effector + Reporter
0.5 cm
(i)
REN
LUC
LUC/REN ratios
(j)
35S::Flag
35S::PdeWRKY6:Flag
Relative enrichment
F1
F2
F3
F4
(k)
Probe
tttgactgtttgactcgttgactg
mProbe
ttccctgttggggtcgtaaaatg
PdeWRKY6
Competitor
10×
100×
Bound probe
Free probe

Figure 7

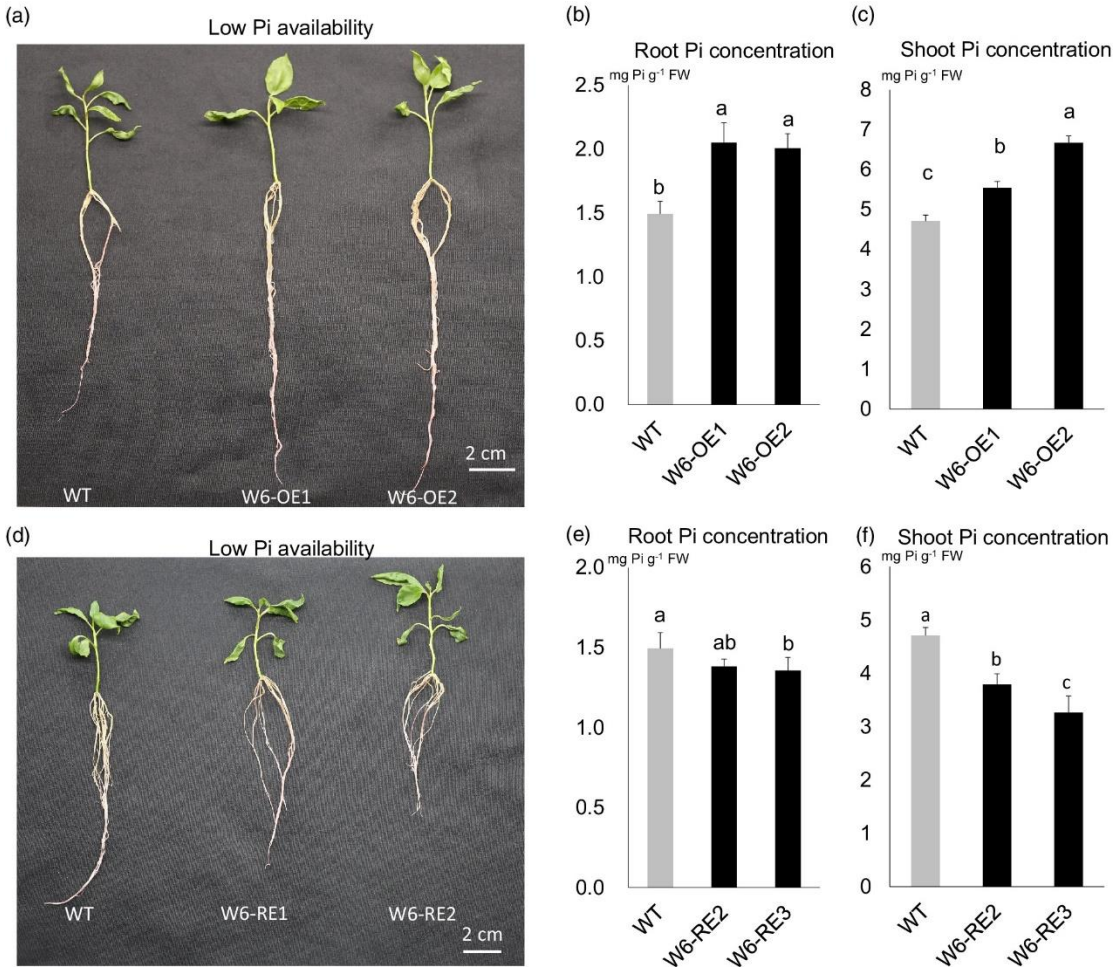
(a)
Low Pi availability
WT
W6-OE1
W6-OE2
2 cm
(b)
Root Pi concentration
mg Pi g-1 FW
(c)
Shoot Pi concentration
mg Pi g-1 FW
(d)
Low Pi availability
WT
W6-RE1
W6-RE2
2 cm
(e)
Root Pi concentration
mg Pi g-1 FW
(f)
Shoot Pi concentration
mg Pi g-1 FW

Figure 8

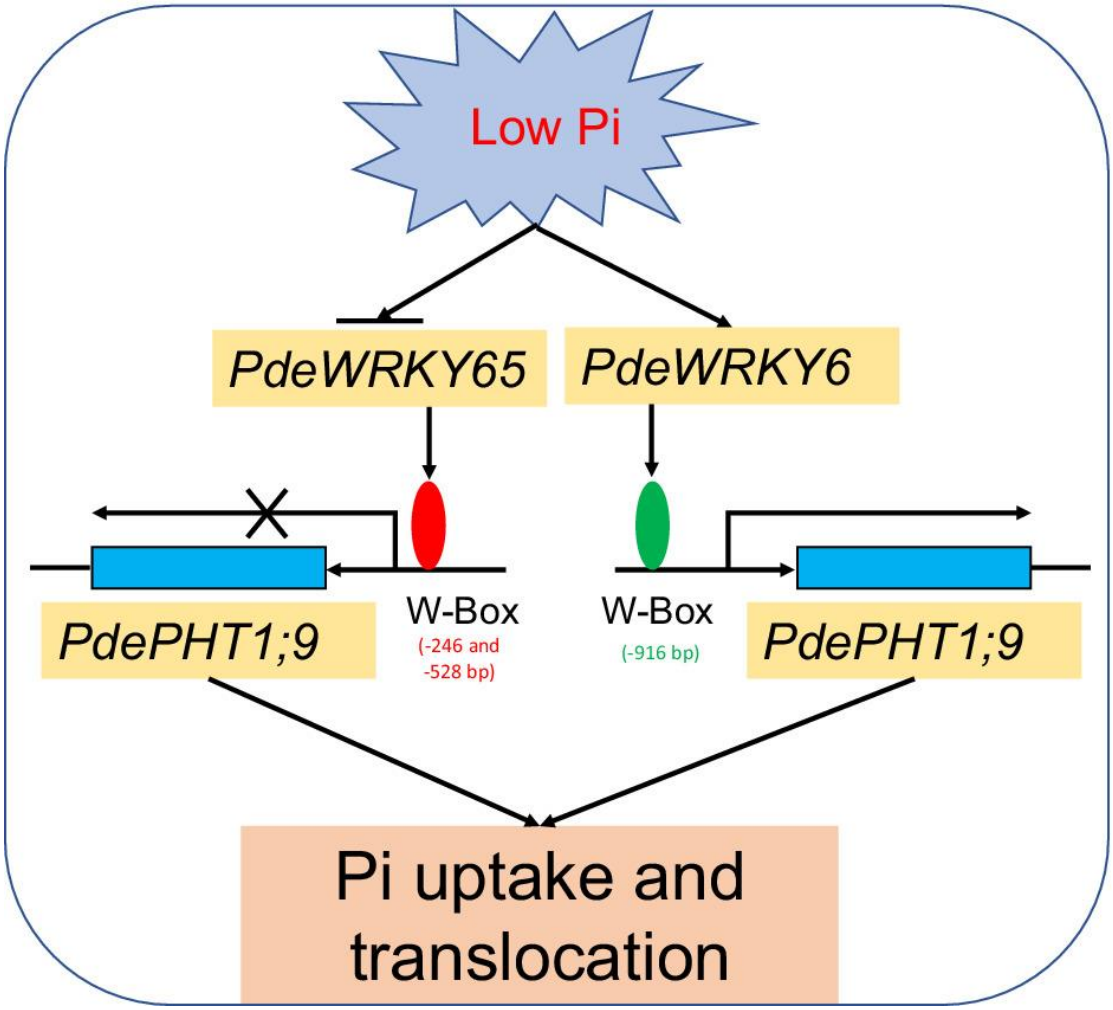
Low Pi
PdeWRKY65
PdeWRKY6
W-Box
(-246 and
-528 bp)
W-Box
(-916 bp)
PdePHT1;9
PdePHT1;9
Pi uptake and
translocation